The Company of **Biologists**

RESEARCH ARTICLE

Error-prone meiotic division and subfertility in mice with oocyte-conditional knockdown of pericentrin

Claudia Baumann[1], Xiaotian Wang[1], Luhan Yang[1] and Maria M. Viveiros[1,2,*]

ABSTRACT

Mouse oocytes lack canonical centrosomes and instead contain unique acentriolar microtubule-organizing centers (aMTOCs). To test the function of these distinct aMTOCs in meiotic spindle formation, pericentrin (Pcnt), an essential centrosome/MTOC protein, was knocked down exclusively in oocytes by using a transgenic RNAi approach. Here, we provide evidence that disruption of aMTOC function in oocytes promotes spindle instability and severe meiotic errors that lead to pronounced female subfertility. Pcnt-depleted oocytes from transgenic (Tg) mice were ovulated at the metaphase-II stage, but show significant chromosome misalignment, aneuploidy and premature sister chromatid separation. These defects were associated with loss of key Pcnt-interacting proteins (γ-tubulin, Nedd1 and Cep215) from meiotic spindle poles, altered spindle structure and chromosome–microtubule attachment errors. Live-cell imaging revealed disruptions in the dynamics of spindle assembly and organization, together with chromosome attachment and congression defects. Notably, spindle formation was dependent on Ran GTPase activity in Pcnt-deficient oocytes. Our findings establish that meiotic division is highly error-prone in the absence of Pcnt and disrupted aMTOCs, similar to what reportedly occurs in human oocytes. Moreover, these data underscore crucial differences between MTOC-dependent and -independent meiotic spindle assembly.

KEY WORDS: Oocyte, Meiosis, Spindle, Pericentrin, Microtubule-organizing center, MTOC

INTRODUCTION

Meiotic division errors can disrupt chromosome stability in gametes prior to fertilization and lead to aneuploidy in developing embryos, which is a major cause of congenital disorders and pregnancy loss in women (Jones and Lane, 2013; Nagaoka et al., 2012). Studies support that aneuploidy can be predominantly attributed to errors that occur during the first meiotic division in oocytes and that the frequency of such errors increases with maternal age (Hassold and Hunt, 2001; Nagaoka et al., 2012). The accuracy of chromosome segregation is critically dependent on the formation of an organized bipolar spindle apparatus, and the establishment of correct chromosome–microtubule (MT) interactions. Moreover, spindle formation in mammalian oocytes differs from that in mitosis (Schuh and Ellenberg, 2007), yet the underlying mechanisms that regulate this essential process are not well defined. Notably, a recent

study demonstrated that spindle assembly in human oocytes occurs independently of centrosomes or microtubule-organizing centers (MTOCs), which leads to intrinsic spindle instability and error-prone meiotic division (Holubcová et al., 2015).

Centrosomes typically function in mammalian cells as the primary organizing centers for the formation and anchorage of spindle MTs (Doxsey et al., 2005). These important non-membrane-bound organelles consist of a pair of centrioles, surrounded by a protein matrix of pericentriolar material (PCM) comprised of key proteins, such as γ-tubulin, that are essential for MT nucleation (Raynaud-Messina and Merdes, 2007). Intriguingly, mammalian (human and mouse) oocytes lack centrioles and canonical centrosomes. Centrioles are only present in oogonia and fetal oocytes up to the pachytene stage and are, thus, absent in growing and pre-ovulatory oocytes during meiotic division (Manandhar et al., 2005; Sathananthan et al., 2000; Szollosi et al., 1972). Despite their critical importance to development, only limited analysis of human oocytes is feasible, and the mouse is a commonly used model of study. Interestingly, mouse oocytes do express essential PCM proteins, despite the absence of centrioles (Combelles and Albertini, 2001; Manandhar et al., 2005; Maro et al., 1985). Studies show that mouse oocytes contain unique acentriolar MTOCs (aMTOCs) that functionally nucleate MTs (Ma et al., 2010; Ma and Viveiros, 2014; Schuh and Ellenberg, 2007), although their relative contribution to meiotic spindle assembly is not fully understood. Key aMTOC-associated proteins identified include γ-tubulin, which catalyzes the assembly of spindle MTs, as well as pericentrin (Pcnt) (Combelles and Albertini, 2001; Schuh and Ellenberg, 2007).

Pcnt functions as an integral centrosome-associated scaffolding protein in mammalian somatic cells. It localizes to the PCM where it binds to γ-tubulin and other essential proteins (Delaval and Doxsey, 2010; Zimmerman et al., 2004). Studies demonstrate that Pcnt is necessary for centrosome assembly, maturation and higher-order organization of the PCM (Kim and Rhee, 2014; Lawo et al., 2012; Lee and Rhee, 2011; Mennella et al., 2012). Loss-of-function mutations in the human Pcnt gene (*PCNT*) are causally linked to a rare and severe form of primordial dwarfism (MOPDII), further supporting its central role in cell division (Griffith et al., 2008; Rauch et al., 2008). $Pcnt^{-/-}$ mice show a similar pathology to MOPDII with significant *in utero* growth restriction and developmental defects that can lead to embryonic lethality (Chen et al., 2014). Pcnt is expressed in mouse oocytes, where it localizes specifically to aMTOCs during oocyte growth and throughout the progression of meiotic division (Łuksza et al., 2013; Ma and Viveiros, 2014; Schuh and Ellenberg, 2007). Our previous *in vitro* studies indicate that Pcnt functions as a scaffolding protein in mouse oocytes analogous to its role in mitotic cells, whereby it regulates the accumulation of essential proteins, such as γ-tubulin and the γ-tubulin ring complex (γTuRC)-associated protein Nedd1, at aMTOCs during meiotic division (Ma et al., 2010; Ma and Viveiros,

[1]Department of Physiology and Pharmacology, College of Veterinary Medicine, University of Georgia, Athens, GA 30602, USA. [2]Regenerative Biosciences Center (RBC), University of Georgia, Athens, GA 30602, USA.

*Author for correspondence (viveiros@uga.edu)

C.B., 0000-0002-4647-0839; M.M.V., 0000-0001-9526-8410

2014). In contrast, Pcnt is not detected in human oocytes, where meiotic spindle assembly reportedly occurs in a chromatin-mediated manner driven by the Ran GTPase pathway rather than MTOCs (Holubcová et al., 2015).

In this study, we developed an oocyte-conditional *Pcnt*-knockdown mouse model to test aMTOC-independent spindle formation in mammalian oocytes. Analysis of oocytes from transgenic (Tg) females reveals that in the absence of Pcnt, spindle formation is dependent on Ran GTPase activity and meiotic division is highly error-prone. Notably, Pcnt-depleted oocytes exhibit disruptions in meiotic spindle assembly and organization with significant chromosome errors, similar to human oocytes, resulting in high rates of aneuploidy and poor female fertility. This is the first experimental model to test the underlying mechanisms of spindle formation as reported in human oocytes, and reveals critical differences between MTOC-dependent and -independent systems.

RESULTS
Oocyte-conditional knockdown of Pcnt lowers fertility
In this study, we used a transgenic RNAi approach (Baumann et al., 2010; Ma et al., 2006; Stein et al., 2003; Svoboda et al., 2001) to develop mice in which *Pcnt*, is knocked down exclusively in oocytes. Transgenic (Tg) mice express a stably integrated double-stranded RNA (dsRNA) construct in which the zona pellucida 3 (ZP3) promoter drives expression of a Pcnt hairpin RNA. Histological analysis of ovaries from 4-month-old wild-type (WT) control and Tg females revealed no overt differences in follicle development or oocyte growth (Fig. S1A), and all females responded to gonadotrophin stimulation for oocyte collection and assessment. Quantitative real-time PCR (qPCR) analysis of ovulated oocytes from WT and Tg females confirmed efficient knockdown of *Pcnt* (Fig. S1B) in two established mouse lines, Tg Line-A and Line-F, which were used for all subsequent studies. Importantly, fertility analysis during 6 months (Fig. 1A) demonstrated that Tg females produced significantly fewer ($P<0.05$) viable pups per litter. This decrease was attributed to both a reduction in the total number of pups born as well as an increase in perinatal mortality (∼25% versus 6.5%) within the first 24 h of birth (Table S1).

Oocyte-specific depletion of the Pcnt protein was confirmed by immunofluorescence analysis (Fig. 1B–D). Pcnt is detected at aMTOCs in all WT oocytes, but is absent in Tg oocytes during both prophase-I arrest (germinal vesicle, GV) and metaphase-II (MII). No Pcnt was detected in over 90% of Tg oocytes, with only ∼10% exhibiting a very weak signal. Pcnt loss was oocyte specific, as the surrounding somatic granulosa cells express Pcnt at the centrosomes (Fig. 1Bb; Fig. S1C). In both groups, GV-stage oocytes exhibit a surrounded nucleolus (SN) chromatin configuration associated with global transcriptional silencing (De La Fuente, 2006). All oocytes were ovulated at the MII-stage post gonadotrophin stimulation and no differences in polar body size were noted. However, despite progression to MII, Tg oocytes show highly misaligned chromosomes (Fig. 1Bd). These data demonstrate the establishment of a unique oocyte-conditional *Pcnt* knockdown mouse model and identify a significant role for Pcnt in female fertility.

Pcnt knockdown leads to loss of aMTOC-associated proteins from meiotic spindle poles
Since Pcnt functions as a critical scaffolding protein, we compared the expression and subcellular distribution of known Pcnt-interacting proteins in ovulated WT and Tg oocytes. While total transcript levels did not differ for key aMTOC-associated proteins such as γ-tubulin (encoded by *Tubg1*) and the γTuRC adaptor

protein Nedd1 (*Nedd1*) (Fig. 1E), the protein distribution was significantly disrupted in Tg oocytes. Neither Nedd1 nor centrosome-associated protein Cep215 [also known as Cdk5Rap2 and the homolog of *Drosophila* Centrosomin (Cnn)] are detected at meiotic spindle pole aMTOCs of Pcnt-depleted oocytes in contrast to WT controls (Fig. 1F). We also assessed the distribution of γ-tubulin (Fig. 1G–K; Fig. S2), considering its essential role in MT nucleation. At the GV-stage, WT oocytes show γ-tubulin colocalized with Pcnt at a single aMTOC, while Tg oocytes show no (or very weak) γ-tubulin labeling (Fig. S2), indicating a lack of protein recruitment. γ-Tubulin distribution was also perturbed in mature MII oocytes from Tg females. Ovulated WT oocytes show diffuse γ-tubulin staining along the spindle MTs (Fig. 1Ia) and staining that colocalized with Pcnt at aMTOCs, both at the spindle poles and at distinct cytoplasmic foci (Fig. S2), consistent with previous studies (Ma and Viveiros, 2014). In contrast, γ-tubulin labeling was only detected along the spindle MTs in Tg oocytes (Fig. 1Ib). These data provide direct support that Pcnt function is conserved in mouse oocytes, and indicate that it is required for the localization of several key proteins to aMTOCs. Importantly, loss of Pcnt disrupts aMTOC protein accumulation, but does not perturb γ-tubulin association with the spindle MTs.

Pcnt depletion promotes increased chromosome–MT attachment errors and aneuploidy
Despite progression to MII, following either *in vivo* or *in vitro* maturation (Fig. S3), analysis of chromosome and spindle MT configurations revealed significant meiotic errors in oocytes from Tg females (Fig. 2). A high percentage (∼45%) of ovulated Tg oocytes exhibit misaligned and uncongressed chromosomes at the spindle poles (Fig. 2A,B). Moreover, karyotype analysis (Fig. 2C,D) revealed that almost 50% of ovulated MII eggs from Tg females are characterized by significant errors in ploidy. Approximately 20% of the oocytes show premature separation of sister chromatids (PCCS) and 30% are aneuploid, with the gain or loss of one or two chromosomes. Direct analysis of kinetochore–MT attachments during metaphase-I (Fig. 2E,F) revealed a lower ($P<0.001$) incidence of end-on attachments in Tg oocytes, with significantly increased ($P<0.01$) numbers of unattached kinetochores as well as erroneous merotelic attachments that likely contribute to the errors observed at MII. These data underscore that loss of Pcnt in oocytes promotes inappropriate and/or disrupted kinetochore–MT interactions as well as potential chromosome segregation errors that lead to aneuploidy.

Altered spindle structure and delayed microtubule regrowth in Pcnt-depleted oocytes
We next compared meiotic spindle configurations in ovulated oocytes from WT and Tg females. Quantitative morphometric analysis established that meiotic spindles are significantly shorter with relatively broader poles in ∼80% of Pcnt-depleted oocytes (Fig. 3A,B). Direct measurements confirm reduced ($P<0.001$) spindle length in Pcnt-depleted oocytes (Fig. 3C). While the average pole diameter (Fig. 3D) was also lower, the ratio of pole diameter to the spindle length (Fig. 3E) was higher ($P<0.001$) in Tg oocytes, indicating that meiotic spindle poles are significantly less focused in the absence of Pcnt. Differences in the dynamics of spindle MT regrowth following depolymerization induced by cold treatment (Fig. 3F,G) were also observed between ovulated WT and Tg oocytes. Mature WT oocytes contained a bipolar spindle with aligned chromosomes and Pcnt at the spindle poles. Following incubation at 4°C, only the cold-stable MTs were labeled. Notably, MT regrowth
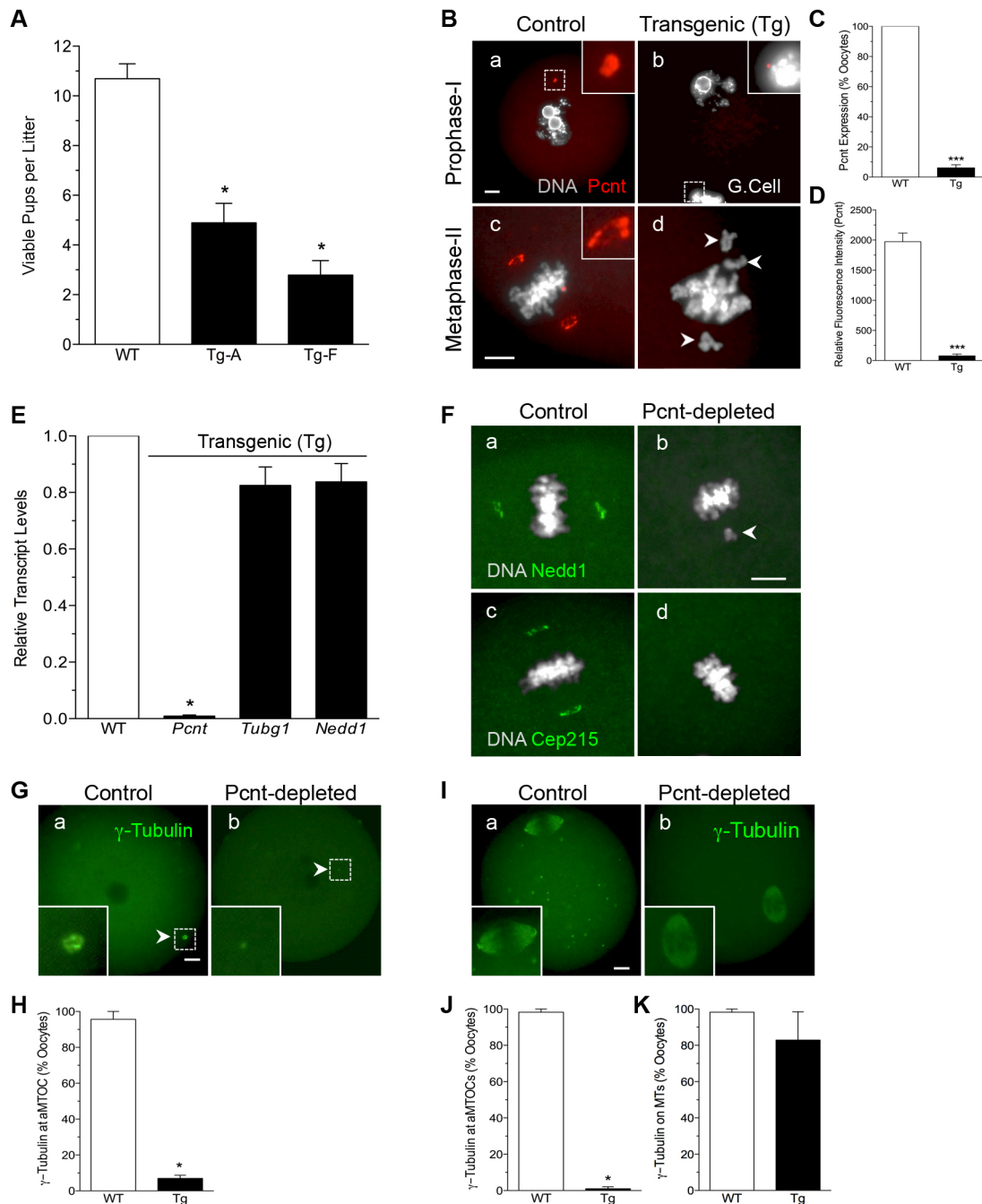
Fig. 1. Oocyte-conditional knockdown of Pcnt disrupts aMTOC-associated protein localization and lowers female fertility. (A) Mean±s.e.m. number of viable pups per litter born to WT (*n*=3) and Tg (*n*=3) female mice mated to WT males during a 6-month period. (B) Representative images of prophase-I (GV-stage) and ovulated oocytes (MII) collected from WT and Tg females. DAPI-labeled DNA is shown in gray and Pcnt in red. Insets show 6× (a) and 3× (b,c) magnifications. Arrowheads denote misaligned chromosomes. G.Cell, granulosa cells. (C) Percentage (mean±s.e.m.) of total WT (*n*=79) and Tg (*n*=61) ovulated MII oocytes that show positive immunofluorescence Pcnt labeling. (D) Fluorescence intensity of Pcnt at aMTOCs in ovulated MII WT (*n*=20) and Tg (*n*=21) oocytes. (E) Relative transcript levels for Pcnt (*Pcnt*), γ-tubulin (*Tubg1*) and the γ-tubulin adaptor protein neural precursor cell expressed, developmentally down-regulated 1 (*Nedd1*) in ovulated oocytes (*n*=100) from control (WT) and transgenic (Tg) females. (F) Representative images of WT and Tg (Pcnt-depleted) oocytes, labeled with anti-Nedd1 (green) or anti-Cep215 (green). DAPI-labeled DNA is shown in gray. Arrowhead denotes misaligned chromosome. Scale bar of 10 μm. (G) Representative images of prophase-1 arrested WT and Tg oocytes, labeled with anti-γ-tubulin (green). The arrowhead denotes an aMTOC. Insets show a 6× magnification. (H) Percentage (mean±s.e.m.) of total WT (*n*=44) and Tg (*n*=42) prophase-I arrested oocytes that label positively for γ-tubulin at aMTOCs. (I) Representative images of ovulated MII WT and Tg oocytes, labeled with anti-γ-tubulin (green). Insets show a 2× magnification. Percentage (mean±s.e.m.) of total WT (*n*=90) and Tg (*n*=98) MII oocytes showing positive labeling for (I) γ-tubulin at the spindle poles and cytoplasmic aMTOC foci, or (J) γ-tubulin along the spindle microtubules (MTs). *P<0.05; ***P<0.001 relative to WT. Scale bars: 10 μm.

was observed in the majority of WT oocytes after rewarming at 37°C for 5 min (Fig. 3G). Similar analysis of Tg oocytes shows the smaller and broader meiotic spindles with no Pcnt. Incubation at 4°C led to

the depolymerization of most MTs, yet cold-stable MTs were still evident in proximity to the spindle poles. However, few Pcnt-depleted oocytes showed MT regrowth after rewarming for 5 min.
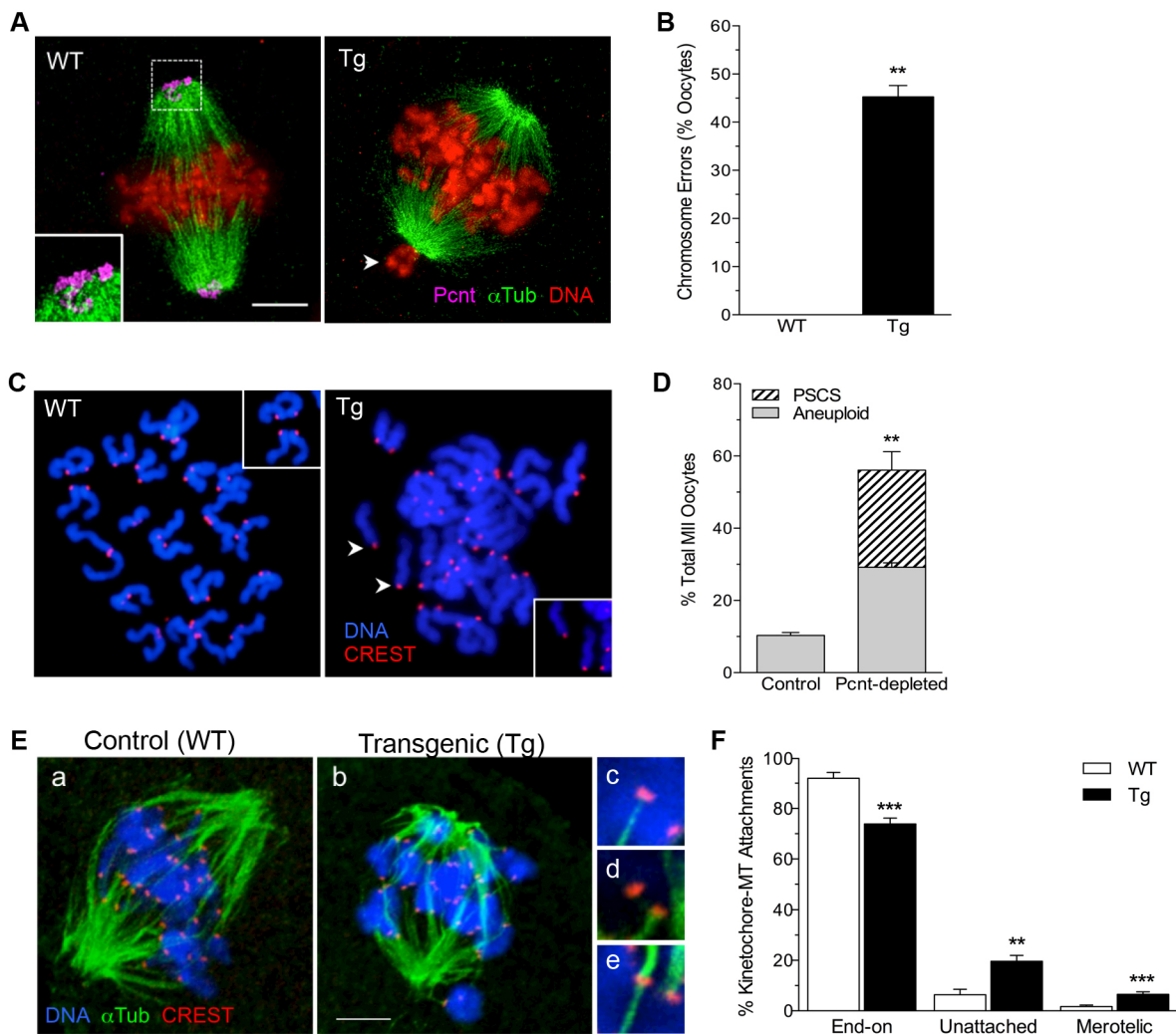
Fig. 2. Loss of Pcnt promotes increased chromosome attachment errors and aneuploidy. (A) Representative images of ovulated MII oocytes from control (WT) and transgenic (Tg) females, labeled with anti-Pcnt (pink) and anti-acetylated α-tubulin (green) to detect spindle MTs. DNA is shown in red. The arrowhead denotes misaligned chromosome at the spindle pole. (B) Percentage (mean±s.e.m.) of total WT (n=32) and Tg (n=52) ovulated oocytes with misaligned chromosomes. (C) Chromosome spreads from WT and Tg (Pcnt-depleted) ovulated MII oocytes. Centromeres (red) were labeled with anti-CREST antibodies and the chromosomes (blue) were counterstained with DAPI. Arrowheads denote prematurely separated sister chromatids (PCCS). (D) Percentage (mean±s.e.m.) of chromosome spreads from WT (n=32) and Tg (n=52) oocytes that show aneuploidy or PCCS. (E) Kinetochore–MT attachments were analyzed in WT (a, n=10) and Tg (b, n=10) MI-stage oocytes. Centromeres (red) are labeled with anti-CREST, MTs (green) with anti-tubulin, and the chromosomes (blue) were counterstained with DAPI. Representative images of (c) end-on, (d) unattached and (e) merotelic attachments are shown. (F) Classification of total WT (n=360) and Tg (n=333) attachments assessed. **P<0.01; ***P<0.001 relative to WT. Scale bars: 10 µm.

These data point to key differences in meiotic spindle assembly in the absence of Pcnt as Tg oocytes contain smaller broad spindles with limited and/or delayed MT regrowth.

Disruption of spindle assembly and chromosome errors during meiotic division in Tg oocytes

Live-cell imaging was used to evaluate the progression of meiosis and dynamics of spindle assembly in real-time between WT (Movie 1) and Tg (Movie 2) oocytes. Time-lapse images were captured at 20-min intervals during a 24 h culture. In both groups, ~85% of oocytes progressed to MII and were analyzed. The majority of WT (n=21) and Tg (n=28) oocytes underwent GV breakdown (GVB) within the first 2 h of culture (Fig. 4A), although Tg oocytes showed a brief but significant (P<0.01) delay in GVB. The timing of subsequent stages is reported as hours (h) post GVB (GVB set to 0 h). Tg oocytes show a pronounced delay (P<0.001) in chromosome congression (Fig. 4B) and a high proportion (42.9%)

exhibit misaligned chromosomes during MI and chromosome lagging during the anaphase–telophase transition (Fig. 4E,F). Notably, these chromosome errors did not cause arrest at MI. While the timing of the anaphase–telophase transition was variable in Tg oocytes, it did not differ significantly between groups (Fig. 4C). At MII, a delay (P<0.01) or failure of chromosome congression on the second meiotic spindle was again noted in Tg oocytes (Fig. 4D).

The observed chromosome errors and perturbed progression of meiosis in Tg oocytes were associated with disrupted meiotic spindle assembly and organization (Fig. 5A). Notably, Tg oocytes are characterized by delays (P<0.01) in the timing of key stages of meiotic spindle formation, including the onset of MT nucleation around the condensing chromosomes upon GVB (Fig. 5B) as well as formation of a growing MT aster during prometaphase (Fig. 5C). Moreover, MT elongation during early MI spindle formation (Fig. 5D) and organization into a bi-polar structure with congressing
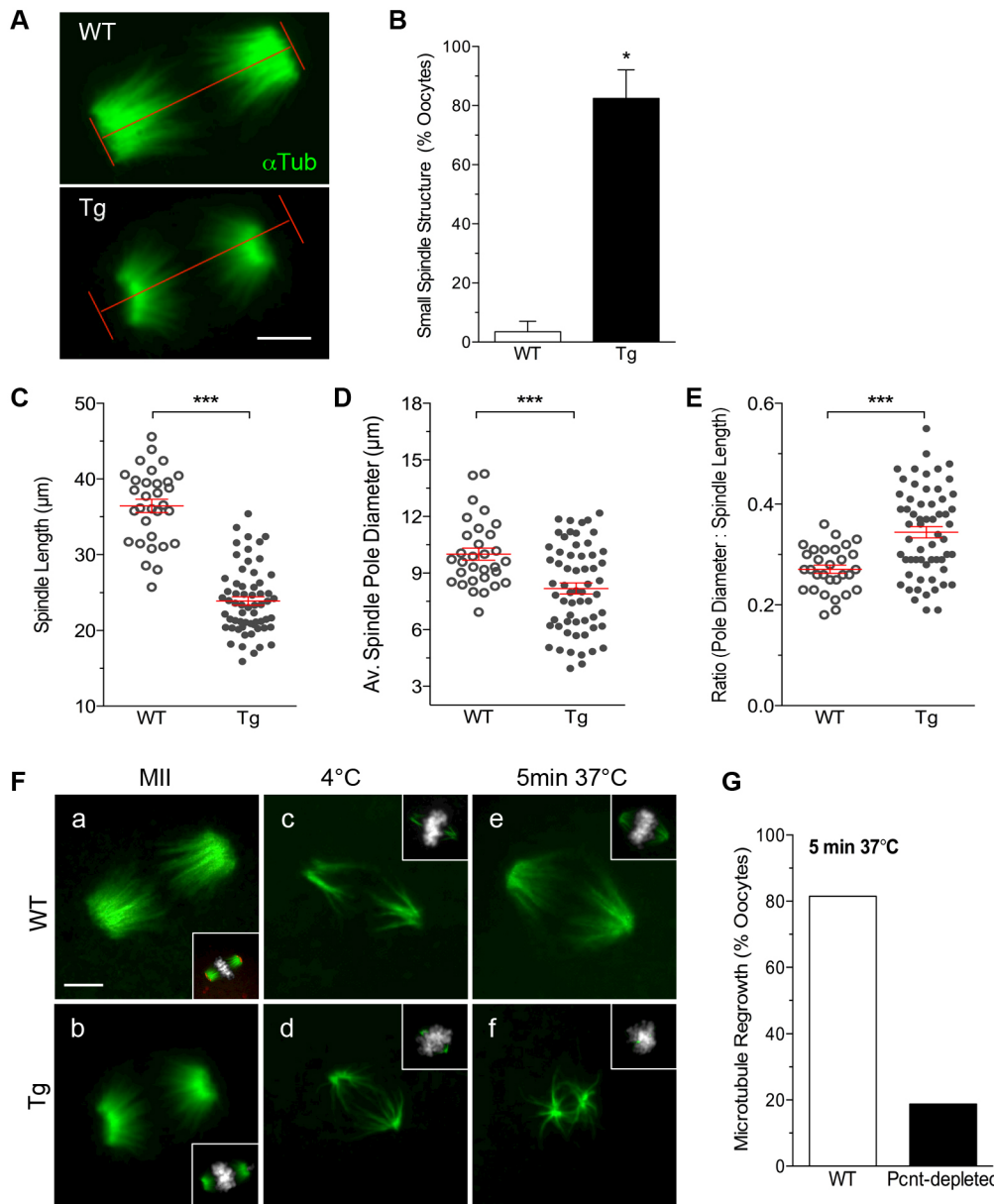
Fig. 3. Loss of Pcnt disrupts meiotic spindle organization and MT re-growth in oocytes.
(A) Representative images of meiotic spindle MTs (green) organization in ovulated WT and Tg oocytes used for morphometric analysis. (B) Percentage (mean±s.e.m.) of spindles that were classified as being smaller in WT (*n*=32) and Tg (*n*=61) oocytes. (C–F) Comparisons of the (mean±s.e.m.) (C) meiotic spindle length, (D) average spindle pole diameter and (E) ratio of the pole diameter:spindle length. (F) Representative images of ovulated WT control (a,c,e; *n*=82) and Tg Pcnt-depleted (b,d,f; *n*=71) oocytes following cold treatment for 1 h at 4°C to depolymerize MTs and microtubule regrowth for 5 min at 37°C. The oocytes were double labeled with anti-Pcnt (red) and anti-acetylated α-tubulin (green) to detect spindle MTs. DNA was counterstained with DAPI (gray). (G) Percentage of oocytes that exhibit MT regrowth after rewarming for 5 min at 37°C. *$P<0.05$; ***$P<0.001$ relative to WT. Scale bars: 10 µm.

chromosomes (Fig. 5E) also occurred later ($P<0.001$) and to a lesser extent, such that MI spindles appeared shorter and broader with misaligned chromosomes in Tg oocytes compared to those in controls. Similarly, organization of the second meiotic spindle into a bi-polar structure after anaphase-I was highly variable and occurred later ($P<0.01$) in Tg oocytes (Fig. 5F). During MII, the Tg oocytes are characterized by a high incidence (~55%) of misaligned chromosomes with some attaching at the spindle poles (Fig. 5G), consistent with the observations in the analysis of fixed oocytes. These data demonstrate that disruption of aMTOC function significantly perturbs meiotic spindle assembly and organization.

Spindle formation is dependent on Ran GTPase activity in Pcnt-depleted oocytes

The Ran-GTP pathway plays an important role in promoting MT nucleation in cells lacking canonical centrosomes (Caudron et al., 2005; Kaláb et al., 2006; Khodjakov et al., 2000). This alternative mechanism is functional in mouse oocytes (Dumont et al., 2007; Schuh and Ellenberg, 2007), and reportedly plays a primary role in

human oocytes (Holubcová et al., 2015). Hence, we tested the potential role of Ran-GTP in meiotic spindle assembly in Pcnt-depleted oocytes (Fig. 6; Movie 3). Ran activity was blocked in Tg oocytes using a dominant-negative mutant of Ran, RanT24N, (Carazo-Salas et al., 2001; Holubcová et al., 2015), and spindle assembly was assessed using live-cell imaging. The Tg oocytes that did not receive RanT24N (*n*=12), showed spindle assembly defects and chromosome errors, as previously observed (Fig. 6A). Strikingly, all Tg RanT24N-injected oocytes (*n*=15) exhibited either no, or significantly delayed, onset of MT nucleation (Fig. 6A–C) upon the resumption of meiosis (GVB set to 0 h). While additional studies are needed to comprehensively assess the relative contribution of Ran activity, these data indicate that meiotic spindle assembly in oocytes is dependent on Ran GTPase activity in the absence of Pcnt and disrupted aMTOC function.

DISCUSSION

In this study, we developed an oocyte-conditional *Pcnt*-knockdown mouse model to test aMTOC-independent spindle formation in
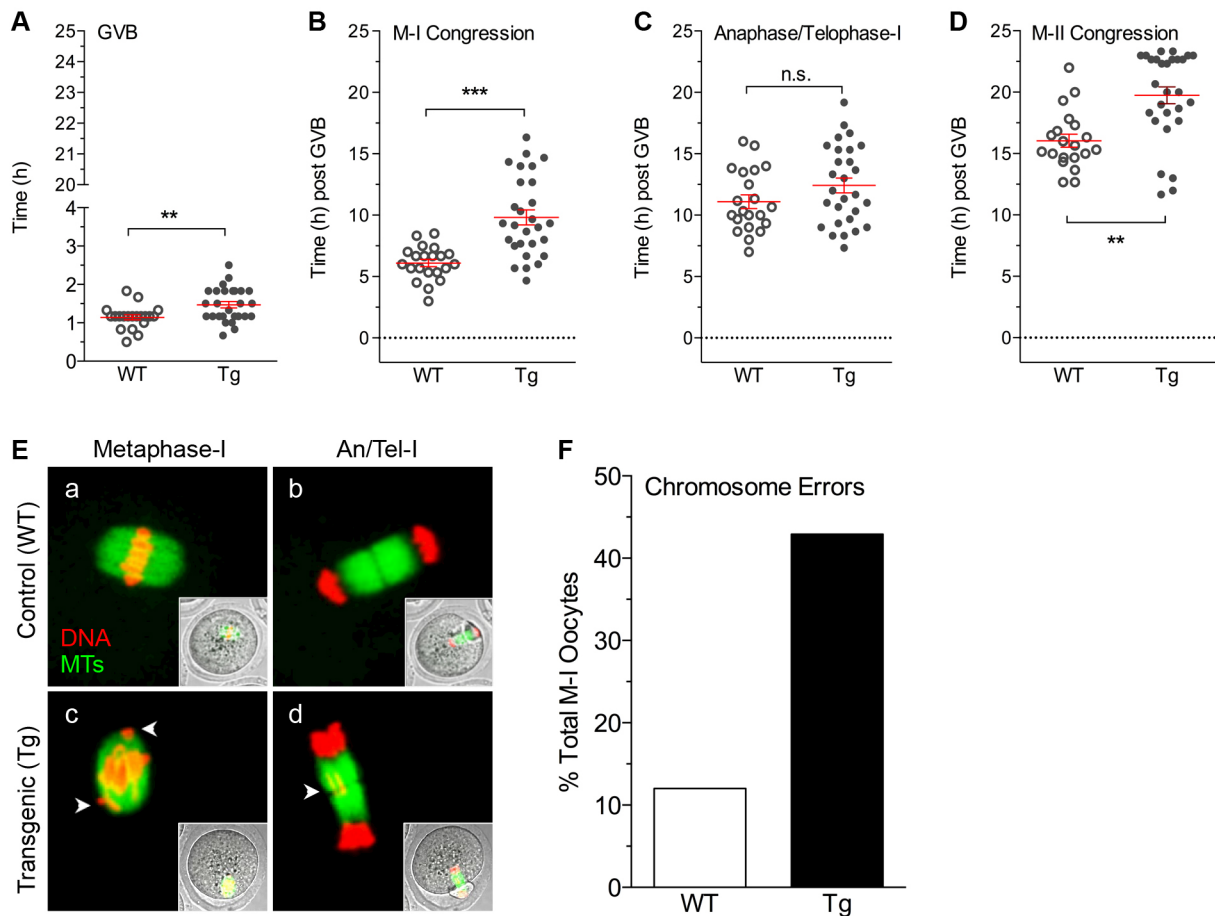
Fig. 4. Progression of meiosis in WT and Tg oocytes as assessed by live-cell imaging. Quantification of the timing of meiotic progression in live WT (*n*=21) and Tg (*n*=28) oocytes expressing H2B–RFP and MAP4–EGFP, which label the chromosomes (red) and spindle MTs (green), respectively. Scatter plots represent the mean±s.e.m. time (h) during which oocytes undergo key transitions including, (A) GVB and the resumption of meiosis, (B) chromosome congression at MI, (C) chromosome segregation at the anaphase–telophase-I transition and (D) chromosome congression at MII. **P<0.01; ***P<0.001; n.s., not significant relative to WT. (E) Representative time-lapse images (maximum intensity z-projections, 5 µm intervals, 100 µm range) of WT and Tg oocytes at MI and at the anaphase–telophase-I transition. Arrowheads denote misaligned or lagging chromosomes. (F) Percentage of oocytes that show misaligned chromosomes during meiosis I.

mammalian oocytes. Our analysis reveals that loss of functional aMTOCs leads to highly error-prone meiotic division and severely reduced female fertility.

Loss of Pcnt disrupts aMTOC-associated proteins
Depletion of Pcnt results in the loss of key MTOC-associated proteins from meiotic spindle poles, including γ-tubulin and the γTuRC adaptor protein Nedd1, which play an essential role in MT nucleation (Lüders et al., 2006; Raynaud-Messina and Merdes, 2007). These data are consistent with our previous *in vitro* analysis (Ma et al., 2010; Ma and Viveiros, 2014) and demonstrate that Pcnt functions as an essential scaffolding protein at aMTOCs in mouse oocytes in an analogous manner to its function in canonical centrosomes (Delaval and Doxsey, 2010; Zimmerman et al., 2004). Our findings also indicate that Pcnt is required for the recruitment of Cep215 (Cdk5Rap2), the homolog of *Drosophila* Cnn (Kim and Rhee, 2014), to aMTOCs. Cep215 together with ninein and centriolin were identified as a subset of key proteins that are targeted to mitotic spindle poles by Pcnt, and play an important role in MT anchoring as well as the formation of mature spindle poles in somatic cells (Chen et al., 2014). Loss of this complex in *Pcnt*^{−/−} embryonic fibroblasts disrupts astral MT formation and attachment to the cell cortex, leading to significant spindle misorientation

(Chen et al., 2014). In contrast, Pcnt-depleted oocytes show no overt defects in spindle orientation and polar body formation, as the meiotic spindle is normally devoid of astral MTs and spindle positioning is instead dependent on the actin network (Azoury et al., 2008; Leader et al., 2002). This underscores key differences between mitotic and meiotic spindle formation and the potential function of aMTOC-associated proteins.

Disruption of aMTOCs leads to error-prone meiotic division
Disruption of aMTOCs does not block the resumption of meiosis and progression to MII; however, Pcnt-depleted oocytes are characterized by significant chromosome errors, such as misaligned and uncongressed chromosomes at the spindle poles, as well as spindle defects. Karyotype analysis showed high rates of aneuploidy and premature separation of sister chromatids in ovulated MII-stage Tg oocytes, indicative of chromosome segregation errors during the first meiotic division. Direct assessment of kinetochore–MT interactions during MI confirmed an increased incidence of unattached kinetochores as well as erroneous merotelic attachments in the Pcnt-depleted group. Live-cell imaging also revealed prevalent chromosome errors throughout the progression of meiosis in Tg oocytes, including disrupted chromosome congression at MI and lagging chromosomes during
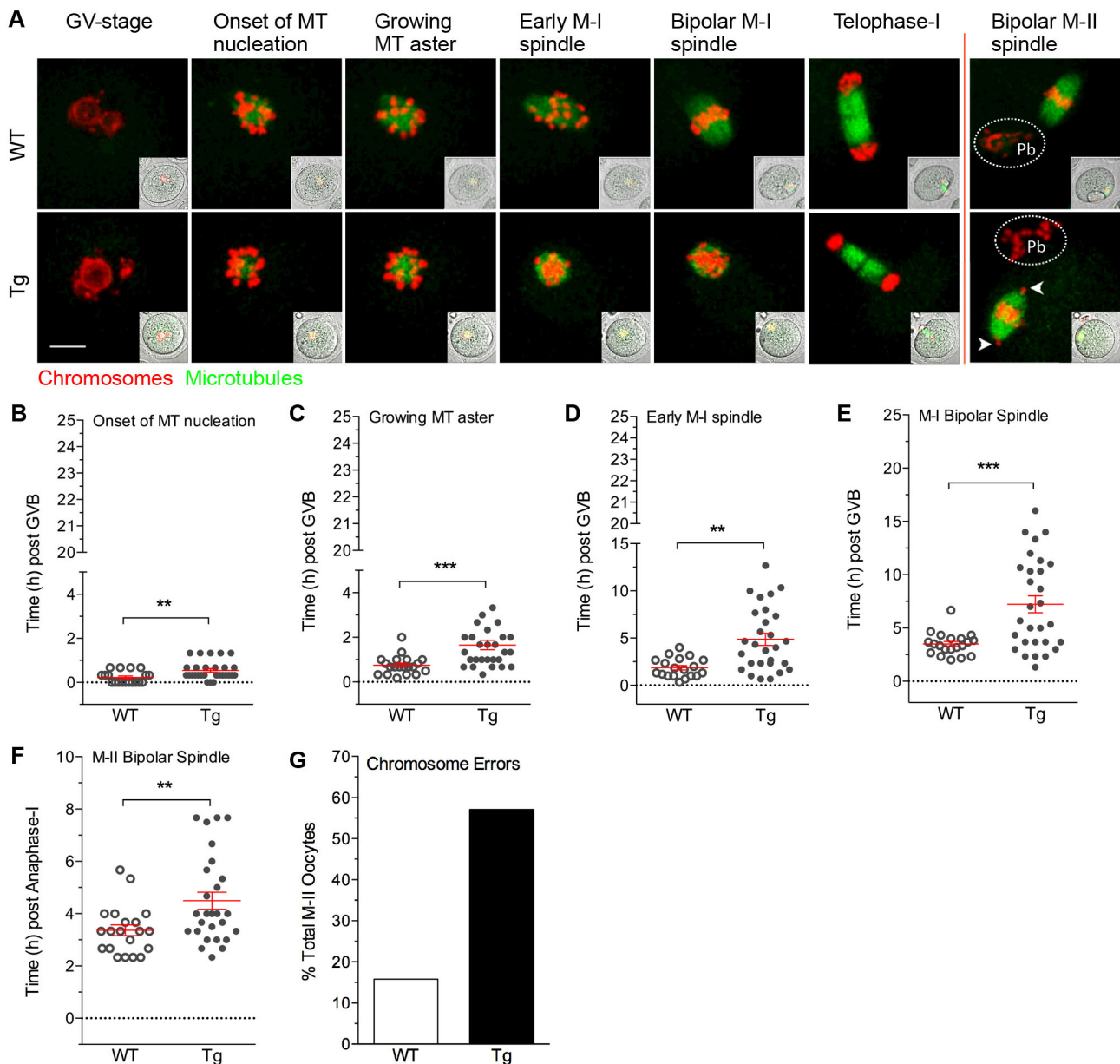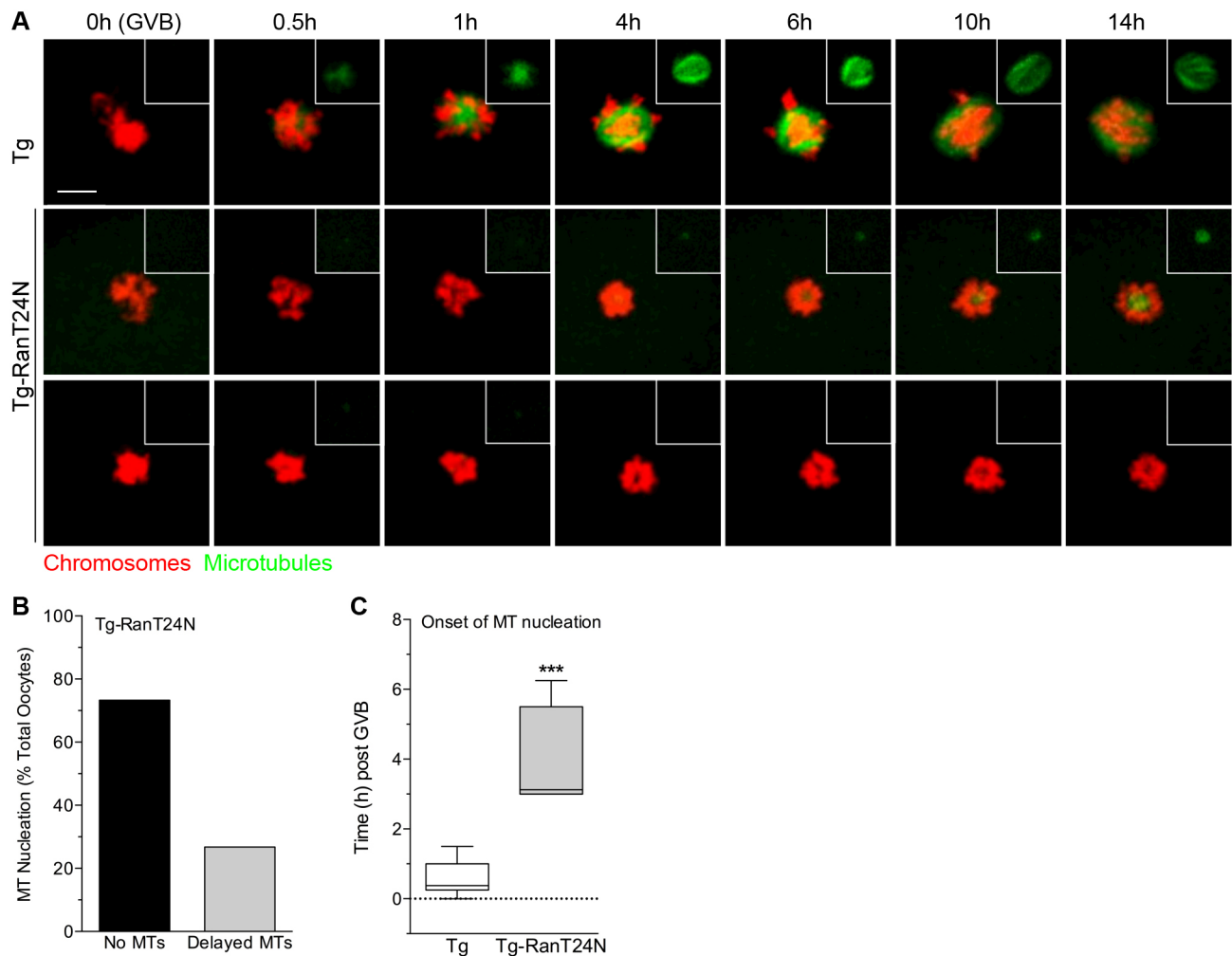
Fig. 5. Meiotic spindle assembly in WT and Tg oocytes as assessed by live-cell imaging. Meiotic spindle assembly and organization was assessed during meiotic division in live oocytes. (A) Time-lapse images (maximum intensity z-projections, 5 μm intervals, 100 μm range) showing key stages of meiosis in WT (n=21) and Tg (n=28) oocytes expressing H2B–RFP and MAP4–EGFP that label the chromosomes (red) and spindle MTs (green), respectively. Arrowheads denote misaligned chromosomes. Pb, polar body. Scale bar: 10 μm. (B–F) Scatter plots represent the mean (±s.e.m) time (h) during which oocytes undergo key stages of spindle MT organization as shown in A, including: (B) onset of MT nucleation around the condensing chromosomes, (C) growing MT-aster formation during prometaphase-I, (D) formation of the early MI spindle, (E) bipolar spindle formation during MI, as well as (F) bipolar spindle formation during MII. (G) Percentage of oocytes that show misaligned chromosomes at MII. **$P<0.01$; ***$P<0.001$ relative to WT.

the anaphase–telophase transition. Mitotic cells that lack functional centrosomes are similarly characterized by delayed chromosome congression, which is attributed to a deficiency in polar ejections forces that are needed to promote chromosome movement toward the spindle equator (Moutinho-Pereira et al., 2013).

Despite overt chromosome–MT attachment defects, the onset of anaphase-I was not significantly delayed in Tg oocytes; this indicates that the spindle assembly checkpoint (SAC) is silenced in these cells. In mitotic cells, the SAC functions as a critical surveillance mechanism that signals a delay in anaphase onset until all chromosomes are appropriately attached to spindle MTs at the kinetochore (Musacchio and Salmon, 2007). However, the high

incidence of aneuploidy in ovulated Tg oocytes demonstrates that the SAC did not effectively detect and/or correct erroneous chromosome–MT interactions during meiosis I. Moreover, the presence of prematurely separated sister chromatids in ovulated Tg oocytes also points to potential deficiencies in chromatid cohesion and/or SAC functioning at MII in the absence of aMTOCs, and warrants further analysis (Lister et al., 2010; Yun et al., 2013). The basis of inefficient SAC function in oocytes is not fully understood, although it has been proposed that the SAC is potentially silenced during MI by the tension applied between the kinetochores of paired homologous chromosomes and that SAC activity has a low threshold for silencing in oocytes (Kitajima et al., 2011; Kolano

Fig. 6. Spindle assembly in Tg (Pcnt-depleted) oocytes is dependent on Ran activity. Meiotic spindle assembly was assessed by live-cell imaging in Tg oocytes microinjected with a mutant form of Ran (RanT24N) and compared to that seen in Tg controls. (A) Representative time-lapse images (maximum intensity z-projections, 5 µm intervals, 100 µm range) showing key stages of meiosis-I in Tg (n=12) and Tg RanT24N-injected (n=15) oocytes expressing H2B–RFP and MAP4–EGFP, which label the chromosomes (red) and spindle MTs (green), respectively. Scale bar: 10 µm. (B) Percentage of Tg-RanT24N oocytes that show either no MT formation, or late onset of MT nucleation, around the condensing chromosomes upon the resumption of meiosis. (C) Time (h) post GVB of MT nucleation onset in Tg and Tg-RanT24N oocytes. GVB was set to 0 h. The box represents the 25–75th percentiles, and the median is indicated. The whiskers show the minimum to maximum time (h). ***P<0.001.

et al., 2012; Kouznetsova et al., 2007; Lane et al., 2012). However, it is also plausible that loss of Pcnt may promote disruptions that limit the capacity of oocytes to correct inappropriate chromosome–MT attachments (Kitajima et al., 2011; Yoshida et al., 2015). For example, spindle MT regrowth was delayed and/or diminished in Tg oocytes following cold treatment, which could potentially influence the frequency and/or stability of kinetochore–MT interactions. Hence, this model may provide important insight into potential differences between aMTOC-dependent and -independent regulation of MT dynamics, kinetochore capture and correction of erroneous MT attachments that contribute to meiotic errors.

Meiotic errors in Tg oocytes are associated with defects in spindle assembly and organization

Loss of Pcnt leads to the formation of shorter meiotic spindles with less-well focused poles. This altered spindle structure supports the idea that Pcnt plays a role in MT anchoring and focusing of meiotic spindle poles. Moreover, it points to potential differences in MT dynamics and the associated proteins that regulate MT length (Bowne-Anderson et al., 2015; Reber et al., 2013) between MTOC-

dependent and -independent spindle assembly. Live-cell imaging revealed significant delays in MT nucleation around the condensing chromosomes as well as disruption of spindle elongation and organization into a bi-polar structure that resulted in shorter broad spindles. Spindle size/organization was variable with some Tg oocytes failing to form a distinct bipolar structure and retaining a rounded (apolar) configuration. These spindle defects are similar to the disrupted spindle formation described in human oocytes, which do not express Pcnt (Holubcová et al., 2015).

Notably, our studies demonstrate that in the absence of Pcnt and aMTOC disruption in oocytes, meiotic spindle assembly is dependent on Ran GTPase activity. In somatic cells, the Ran GTPase pathway functions as an important alternative MT-generating mechanism that supports centrosome-independent spindly assembly by promoting MT nucleation and organization around the condensing chromosomes (Caudron et al., 2005; Kaláb et al., 2006; Khodjakov et al., 2000). Ran activity has also been shown to promote MT nucleation in mouse oocytes, although its relative contribution to meiotic spindle formation during MI and MII is not fully understood (Dumont et al., 2007; Hinkle et al.,

2002; Schuh and Ellenberg, 2007). Ran reportedly functions as the primary mechanism that promotes spindle formation in human oocytes, which lack Pcnt (Holubcová et al., 2015). Similar to human oocytes, γ-tubulin was observed around the chromosomes in Tg oocytes and blocking of Ran activity significantly delayed or inhibited MT nucleation upon the resumption of meiosis. Future studies are, thus, warranted for a more comprehensive analysis of Ran function in mouse oocytes.

Analysis of Tg (Pcnt-depleted) oocytes demonstrates that aMTOCs play a pivotal role in the assembly and organization of a bipolar meiotic spindle in mouse oocytes. While Ran-mediated MT nucleation functions as an important alternative pathway for MT nucleation, alone it did not support stable meiotic spindle formation, leading to error-prone meiotic division and reduced fertility. Therefore, an important question is why human oocytes behave differently from mouse oocytes, such that these cells can lack Pcnt and functional aMTOCs and still support proper meiotic spindle assembly. It is somewhat perplexing considering that Pcnt is highly conserved across species and numerous cell types (Delaval and Doxsey, 2010). One key consideration is that since mammalian female gametes originate during fetal development, human oocytes remain arrested for many years compared to the much shorter-lived mouse oocyte. However, whether maternal age is a contributing factor to the absence of Pcnt in human oocytes is not known. The quality of the oocyte may also be an important factor, as the human oocytes used for analysis were obtained from patients undergoing assisted reproductive technologies and did not resume meiosis in response to hormone stimulation (Holubcová et al., 2015).

In summary, our findings establish that Pcnt is a key conserved and essential component of the unique aMTOCs in mouse oocytes, which play a vital role in meiotic spindle assembly and stability. Oocyte-conditional knockdown of *Pcnt* disrupts aMTOCs and spindle formation, leading to highly error-prone meiotic division and patent female subfertility. Notably, Pcnt-depleted oocytes from Tg female mice show strikingly similar spindle assembly and chromosome errors to human oocytes, which lack detectable aMTOCs and depend on Ran activity for MT nucleation. This provides a unique mechanistic model to study the underlying molecular basis of meiotic errors that promote chromosome abnormalities and congenital disorders.

MATERIALS AND METHODS
Pcnt dsRNA construct design and generation of transgenic animals
All studies were undertaken in accordance with the Institutional Animal Care and Use Committee (IACUC) at the University of Georgia. Oocyte-conditional knockdown of Pcnt was achieved using a transgenic RNAi approach. Transgenic (Tg) animals were generated that carry a stably integrated dsRNA construct, which drives the synthesis of a Pcnt hairpin and enhanced green fluorescent protein (EGFP) under control of the ZP3 promoter. The Pcnt hairpin was cloned into an established pZP3-intron-EGFP vector (Baumann et al., 2010; Ma et al., 2006; Stein et al., 2003; Svoboda et al., 2001). For cloning the inverted repeat, a Pcnt-specific coding sequence spanning exons 24 and 25 was amplified from C57Bl/6J mouse oocyte cDNA using a primer pair containing BglII and *XbaI* restriction sites (Pcnt-fwd1, 5′-AGATCTGGTG-AAGAAAGTAAGGCCATCGCC-3′ and Pcnt-rev, 5′-TCTAGAACTTTT-CCTGCTCCCATCGC-3′). A shorter fragment was also amplified using the primer pair Pcnt-fwd2, 5′-GGATCCGTGGACCTTTCTCTTCCCAAGC-3′ and Pcnt-rev. Both PCR amplicons were sub-cloned into pCR4-TOPO (Invitrogen, Carlsbad, CA) before *NotI/BglII* excision of the longer hairpin fragment and insertion into the *BamHI/Not1*-linearized vector carrying the shorter hairpin fragment. Following XbaI digest, the inverted repeat was inserted into the pZP3-intron-EGFP vector to generate

pZP3-intron-EGFP-Pcnthp. Microinjection of the transgenic construct into pronuclear stage embryos was conducted at the Mouse Transgenic and Gene Targeting Core (Emory University School of Medicine). Tg mice were identified by standard PCR using the primer pair EGFPseq-F, 5′-AAAGACCCCAACGAGAAGCG-3′ and Pcnt-fwd2, or through the presence of a 301 bp amplicon originating from an SV40 intron as described previously (Stein et al., 2003). An additional primer pair (CNTL-fwd, 5′-ATGGCCACTGTAGGTTCAGC-3′ and CNTL-rev, 5′-CCTGAAGTTCACGGAAAAGC-3′) was used as an internal control. A total of 11 founder mice were identified with successful transgene integration, of which nine survived. From these founders, three males and one female were successfully bred to CF1 control mice and analysis of the F1 progeny demonstrated efficient germline transmission of the transgene. Transgenic (Tg) F1 males were used for successive backcrossing with CF1 females for up to seven generations to establish four unique Tg mouse lines (identified as Lines-A, -C, -E and -F).

Fertility analysis
To assess fertility, WT control (n=3) and Tg (n=3) females from two key established mouse lines with efficient *Pcnt* knockdown in oocytes (Line-A and Line-F) were mated with CF1 males at a ratio of 1:1. Mating pairs were continuously housed together for a period of 6 months, to assess parturition frequency and the number of pups born per litter.

Oocyte collection and culture
Oocytes were collected from pre-ovulatory stage follicles for analysis as described previously (Ma and Viveiros, 2014). Prophase-I-arrested (GV-stage) oocytes were recovered from the ovaries of 22–24-day-old females 44 to 48 h after injection with 5 IU of pregnant mare serum gonadotropin (PMSG; National Hormone & Peptide Program). Oocytes were collected in minimal essential medium (MEM) supplemented with 3 mg/ml bovine serum albumin (MEM/BSA; Sigma-Aldrich), and 10 μM Milrinone (Sigma-Aldrich) to prevent GV breakdown. *In vitro*-matured MII oocytes were obtained following culture of cumulus-enclosed GV-stage oocytes in fresh MEM/BSA medium supplemented with 5% fetal bovine serum (FBS, Hyclone, Atlanta Biologicals) for 17 h under an atmosphere of 5% O_2, 5% CO_2 and 90% N_2 at 37°C. Ovulated (*in vivo* matured) MII oocytes were collected from the oviducts of females treated with 5 IU PMSG followed by 5 IU human chorionic gonadotropin injection (hCG; EMD Biosciences, Inc., La Jolla, CA) 44–48 h later. The oviducts were collected for oocyte recovery 15 h post hCG injection.

qPCR
mRNA was isolated from groups of 100 denuded oocytes using the RNeasy micro kit (Qiagen) and reverse transcribed using the RT² First Strand Kit (Qiagen) according to manufacturer's recommendations. The resultant cDNA was used for qPCR with validated gene-specific RT² qPCR primers (Qiagen) in combination with the RT² SYBR Green PCR Master Mix (Qiagen) on a RotorGene Q100 light cycler apparatus (Qiagen). Validated qPCR primers were purchased from Qiagen to assess transcript levels for Pcnt (*Pcnt*), γ-tubulin (*Tubg1*) and the γTuRC adaptor protein Nedd1 (*Nedd1*). qPCR results were normalized against *GAPDH* transcript levels as a housekeeping control. Raw threshold cycle data obtained from control and Tg oocyte samples were analyzed using RT² Profiler PCR Array Data Analysis software version 3.5 (SA Biosciences; Qiagen) to conduct all ΔΔCt-based calculations.

Immunochemistry
Ovaries from 4-month-old WT and Tg females were fixed in Bouin's solution and processed for paraffin sectioning (5 μm) and hematoxylin & eosin staining using standard procedures. Oocyte samples were washed in MEM/BSA and fixed with 4% paraformaldehyde (PFA) and 0.1% Triton-X for 30 min at 37°C, then rinsed and transferred to phosphate-buffered saline (PBS) supplemented with 5% serum for 24 h at 4°C prior to immunostaining as previously described (Baumann and Viveiros, 2015; Ma and Viveiros, 2014). Antibodies were used at a 1:1000 dilution to detect Pcnt (BD Biosciences and Covance, cat# PRB-432C), γ-tubulin (Sigma,

cat# T3559), Nedd1 (Novus Biologicals, cat# H00121441-M05) and Cep215 (EMD, Millipore, cat# ABE236) as well as spindle MTs with acetylated α-tubulin (Sigma, cat# T6793, clone 6-11B-1). Immunodetection was performed using specific Alexa Fluor 488- and 555-conjugated secondary antibodies (Thermo Fisher, cat# A-11017, A-21430, A-11070, A-21425) at a dilution of 1:1000 during a 1 h incubation at room temperature. After the final wash, the cells were transferred onto glass slides and overlaid with mounting medium (VectaShield, Vector Laboratories, Burlingame, CA) containing 4′,6-diamidino-2-phenylindole (DAPI) to counterstain the DNA. Fluorescence was assessed using an upright fluorescent microscope with imaging software (Leica Microsystems). Spindle measurements of ovulated MII oocytes were obtained using a Leica DFC 350F camera and the measurements module of Openlab 3.1.7 image analysis software (Improvision Inc.) by determining the spindle length (distance between spindle poles) as well as the spindle pole diameter (pole width).

Chromosome analysis

MII oocytes were recovered from the oviducts of control and Tg female mice for chromosome analysis to determine ploidy. The surrounding cumulus cells were removed in MEM/BSA medium supplemented with hyaluronidase (Sigma-Aldrich). Surface spread chromosomes from individual oocytes were prepared following removal of the surrounding zona pellucida with a brief exposure to acid Tyrode's solution (Sigma). Zona-free oocytes were allowed to recover for 5 min in MEM/BSA, then spread on clean glass slides in a solution of 1% PFA with 0.1% Triton X-100 as described previously (Baumann et al., 2010). For immunochemistry, centromeres were labeled with a 1:500 dilution of anti-CREST antiserum (Nuclear ANA-Centromere Autoantibody, Cortex Biochem, Concord, MA, cat# CS1058) during an overnight incubation at 4°C. Following three 10-min washes in PBS/BSA, the slides were incubated with a 1:1000 dilution of Alexa Fluor 555-conjugated secondary antibody (ThermoFisher) for 1 h at room temperature. The chromosomes were counterstained with DAPI supplemented mounting medium (Vecta Shield plus DAPI, Vector Laboratories, Inc., Burlingame, CA).

Kinetochore-microtubule attachment analysis

Oocytes were processed for kinetochore–MT attachment analysis as previously described (Davydenko et al., 2013). In brief, MI-stage oocytes (∼6.5 h post GVB) were cold treated at 4°C for 10 min to depolymerize the spindle MTs then fixed immediately in 4% PFA. Prior to immunochemistry, the oocytes were permeabilized in PBS supplemented with 0.1% Triton X-100 and 0.3% BSA for 15 min at room temperature. Immunochemistry was conducted as described above using Human CREST autoimmune serum (1:500 dilution of Nuclear ANA-Centromere Autoantibody, Cortex Biochem, Concord, MA, cat# CS1058) together with anti-α-tubulin (1:1000; Sigma, cat# T6793, clone 6-11B-1) overnight at 4°C, to label the kinetochores and spindle MTs. Incubation with specific Alexa Fluor 488- and 555-conjugated secondary antibodies (1:1000) was conducted at room temperature for 1 h. After the final wash, the cells were transferred onto glass slides and overlaid with mounting medium (Vecta Shield) containing DAPI to counterstain the DNA. The entire meiotic spindle was visualized by confocal microscopy using a Nikon Eclipse Ti-U/D-Eclipse C1 laser scanning confocal microscope equipped with a 40× oil immersion lens following sequential (frame lambda) excitation with a 488 and 561 nm Coherent Sapphire laser, to detect MTs and kinetochores, respectively. Image acquisition was conducted using EZ-C1 software (Nikon) with a step size of 0.3 μm and a Z-stack range of 11–15 μm. Confocal Z-stacks were subsequently analyzed using NIH Elements software (Nikon) to classify kinetochore–MT attachments layer-by-layer.

Spindle MT regrowth

Spindle MT regrowth was assessed in ovulated oocytes collected from control and Tg females, following MT depolymerization with cold treatment as previously described (Haren et al., 2006; Ma and Viveiros, 2014). Mature MII eggs were recovered from the oviducts of superovulated transgenic and control females 15 h post hCG (5 IU; EMD Biosciences) injection. A representative sample of freshly isolated MII oocytes from each group was

fixed for immunofluorescence analysis, and the remaining oocytes were placed in cold M2 medium (Sigma) at 4°C for 1 h to depolymerize the spindle MTs. After cold treatment, oocytes were transferred to fresh pre-warmed MEM medium at 37°C for MT regrowth, then fixed for immunofluorescence analysis at 0 and 5 min post warming. The oocytes were immunostained with anti-Pcnt and anti-acetylated α-tubulin antibodies as described above, and assessed by using an upright fluorescent microscope with imaging software (Leica Microsystems).

Live-cell imaging

Live-cell imaging was used to compare meiotic spindle assembly during meiotic division in real time between control and Tg oocytes. Time-lapse image acquisition was performed following microinjection of a capped messenger RNA (cRNA) cocktail encoding histone H2B–RFP and MAP4–EGPF fusion proteins into the cytoplasm of fully-grown prophase-I arrested (GV-stage) oocytes in order to visualize the chromosomes (red) and MTs (green), respectively. Capped mRNAs were synthesized from vectors pGEMHE-EGFP-MAP4 and pH2B-mRFP (EUROSCARF) using the T7 mMESSAGE mMACHINE Kit (ThermoFisher) as previously described (Baumann et al., 2010). Following cRNA microinjection, the oocytes were cultured at 37°C overnight in MEM/BSA with 10 μM milrinone to allow recombinant protein expression during prophase-I arrest. The next day, the oocytes were washed in fresh medium with no milrinone and transferred to a 200 μl microdrop of MEM/BSA medium supplemented with 5% FBS under mineral oil within an environmental chamber (Tokai Hit, Fujinomiya, Japan). The temperature was maintained at 37°C in an atmosphere of 5% CO_2, 5% O_2 and balanced N_2. The progression of meiosis as well as the dynamics of spindle assembly and stability were monitored for 24 h by time-lapse microscopy at 20-min intervals using a Nikon Eclipse Ti-U/D-Eclipse C1 laser scanning confocal microscope equipped with a 40× objective lens following sequential (frame lambda) excitation of GFP fusion proteins with a 488 nm Coherent Sapphire laser and RFP fusion proteins with a 561 Coherent Sapphire laser. Image acquisition was conducted using EZ-C1 software (Nikon) with a step size of 5 μm and a Z-stack range of 100 μm. Live-cell imaging data were subsequently analyzed by maximum intensity and 3D reconstructions by using NIH Elements software (Nikon).

Modulation of Ran activity

To test the role of Ran GTPase activity in Pcnt-depleted oocytes, a dominant-negative form of Ran (RanT24N) was microinjected into Tg oocytes as previously described (Holubcová et al., 2015). In brief, prophase-I arrested (GV-stage) oocytes were collected from Tg females and microinjected with H2B–RFP and Map4–EGFP cRNA to label chromosomes and spindle MTs, and were cultured overnight in MEM/BSA at 37°C to allow recombinant protein expression. The medium was supplemented with 10 μM milrinone to maintain prophase-I arrest. The next day, the oocytes were washed in fresh medium with no milrinone and microinjected with a 0.5 μg/μl solution of RanT24N (Cytoskeleton Inc., Cat #: RN05) prepared in nuclease-free water. Following microinjection, the oocytes were transferred to a 200 μl microdrop of MEM/BSA medium supplemented with 5% FBS under mineral oil within an environmental chamber (Tokai Hit, Fujinomiya, Japan) for confocal imaging. Temperature was maintained at 37°C in an atmosphere of 5% CO_2, 5% O_2 and balanced N_2. The progression of meiosis and MT formation were monitored for 14 h by time-lapse microscopy at 15-min intervals using a Nikon Eclipse Ti-U/D-Eclipse C1 as described above.

Statistical analysis

All data are presented as mean percentages (±s.e.m.) of a minimum of three independent experimental replicates. Normal distribution of sample values was analyzed using the D'Agostino and Pearson omnibus normality test (GraphPad Prism 5). For normally distributed samples, P-values were then calculated from two-tailed unpaired t-tests, while nonparametric Mann–Whitney tests were performed on samples that did not pass the D'Agostino & Pearson omnibus normality test (GraphPad Prism 5). Differences were considered significant when $P<0.05$. Unless otherwise stated, P-values are indicated using the following key: *$P<0.05$, **$P<0.01$, ***$P<0.001$.

Author contributions
C.B. and M.M.V. designed the research. C.B., X.W., L.Y. and M.M.V. performed the research as well as the data analysis. M.M.V. wrote the paper.

Supplementary information
Supplementary information available online at
http://jcs.biologists.org/lookup/doi/10.1242/jcs.196188.supplemental

References

Azoury, J., Lee, K. W., Georget, V., Rassinier, P., Leader, B. and Verlhac, M.-H. (2008). Spindle positioning in mouse oocytes relies on a dynamic meshwork of actin filaments. *Curr. Biol.* **18**, 1514-1519.

Baumann, C. and Viveiros, M. M. (2015). Meiotic spindle assessment in mouse oocytes by siRNA-mediated silencing. *J. Vis. Exp.* **104**, e53586.

Baumann, C., Viveiros, M. M. and De La Fuente, R. (2010). Loss of maternal ATRX results in centromere instability and aneuploidy in the mammalian oocyte and pre-implantation embryo. *PLoS Genet.* **6**, e1001137.

Bowne-Anderson, H., Hibbel, A. and Howard, J. (2015). Regulation of microtubule growth and catastrophe: unifying theory and experiment. *Trends Cell Biol.* **25**, 769-779.

Carazo-Salas, R. E., Gruss, O. J., Mattaj, I. W. and Karsenti, E. (2001). Ran-GTP coordinates regulation of microtubule nucleation and dynamics during mitotic-spindle assembly. *Nat. Cell Biol.* **3**, 228-234.

Caudron, M., Bunt, G., Bastiaens, P. and Karsenti, E. (2005). Spatial coordination of spindle assembly by chromosome-mediated signaling gradients. *Science* **309**, 1373-1376.

Chen, C.-T., Hehnly, H., Yu, Q., Farkas, D., Zheng, G., Redick, S. D., Hung, H.-F., Samtani, R., Jurczyk, A., Akbarian, S. et al. (2014). A unique set of centrosome proteins requires pericentrin for spindle-pole localization and spindle orientation. *Curr. Biol.* **24**, 2327-2334.

Combelles, C. M. H. and Albertini, D. F. (2001). Microtubule patterning during meiotic maturation in mouse oocytes is determined by cell cycle-specific sorting and redistribution of γ-tubulin. *Dev. Biol.* **239**, 281-294.

Davydenko, O., Schultz, R. M. and Lampson, M. A. (2013). Increased CDK1 activity determines the timing of kinetochore-microtubule attachments in meiosis I. *J. Cell Biol.* **202**, 221.

De La Fuente, R. (2006). Chromatin modifications in the germinal vesicle (GV) of mammalian oocytes. *Dev. Biol.* **292**, 1-12.

Delaval, B. and Doxsey, S. J. (2010). Pericentrin in cellular function and disease. *J. Cell Biol.* **188**, 181-190.

Doxsey, S., McCollum, D. and Theurkauf, W. (2005). Centrosomes in cellular regulation. *Annu. Rev. Cell Dev. Biol.* **21**, 411-434.

Dumont, J., Petri, S., Pellegrin, F., Terret, M.-E., Bohnsack, M. T., Rassinier, P., Georget, V., Kalab, P., Gruss, O. J. and Verlhac, M.-H. (2007). A centriole- and RanGTP-independent spindle assembly pathway in meiosis I of vertebrate oocytes. *J. Cell Biol.* **176**, 295-305.

Griffith, E., Walker, S., Martin, C.-A., Vagnarelli, P., Stiff, T., Vernay, B., Sanna, N. A., Saggar, A., Hamel, B., Earnshaw, W. C. et al. (2008). Mutations in pericentrin cause Seckel syndrome with defective ATR-dependent DNA damage signaling. *Nat. Genet.* **40**, 232-236.

Haren, L., Remy, M.-H., Bazin, I., Callebaut, I., Wright, M. and Merdes, A. (2006). NEDD1-dependent recruitment of the {gamma}-tubulin ring complex to the centrosome is necessary for centriole duplication and spindle assembly. *J. Cell Biol.* **172**, 505-515.

Hassold, T. J. and Hunt, P. A. (2001). To err (meiotically) is human: the genesis of human aneuploidy. *Nat. Rev. Genet.* **2**, 280-291.

Hinkle, B., Slepchenko, B., Rolls, M. M., Walther, T. C., Stein, P. A., Mehlmann, L. M., Ellenberg, J. and Terasaki, M. (2002). Chromosomal association of Ran during meiotic and mitotic divisions. *J. Cell Sci.* **115**, 4685-4693.

Holubcová, Z., Blayney, M., Elder, K. and Schuh, M. (2015). Error-prone chromosome-mediated spindle assembly favors chromosome segregation defects in human oocytes. *Science* **348**, 1143-1147.

Jones, K. T. and Lane, S. I. R. (2013). Molecular causes of aneuploidy in mammalian eggs. *Development* **140**, 3719-3730.

Kaláb, P., Pralle, A., Isacoff, E. Y., Heald, R. and Weis, K. (2006). Analysis of a RanGTP-regulated gradient in mitotic somatic cells. *Nature* **440**, 697-701.

Khodjakov, A., Cole, R. W., Oakley, B. R. and Rieder, C. L. (2000). Centrosome-independent mitotic spindle formation in vertebrates. *Curr. Biol.* **10**, 59-67.

Kim, S. and Rhee, K. (2014). Importance of the CEP215-pericentrin interaction for centrosome maturation during mitosis. *PLoS ONE* **9**, e87016.

Kitajima, T. S., Ohsugi, M. and Ellenberg, J. (2011). Complete kinetochore tracking reveals error-prone homologous chromosome biorientation in mammalian oocytes. *Cell* **146**, 568-581.

Kolano, A., Brunet, S., Silk, A. D., Cleveland, D. W. and Verlhac, M.-H. (2012). Error-prone mammalian female meiosis from silencing the spindle assembly checkpoint without normal interkinetochore tension. *Proc. Natl. Acad. Sci. USA* **109**, E1858-E1867.

Kouznetsova, A., Lister, L., Nordenskjöld, M., Herbert, M. and Höög, C. (2007). Bi-orientation of achiasmatic chromosomes in meiosis I oocytes contributes to aneuploidy in mice. *Nat. Genet.* **39**, 966-968.

Lane, S. I. R., Yun, Y. and Jones, K. T. (2012). Timing of anaphase-promoting complex activation in mouse oocytes is predicted by microtubule-kinetochore attachment but not by bivalent alignment or tension. *Development* **139**, 1947.

Lawo, S., Hasegan, M., Gupta, G. D. and Pelletier, L. (2012). Subdiffraction imaging of centrosomes reveals higher-order organizational features of pericentriolar material. *Nat. Cell Biol.* **14**, 1149-1158.

Leader, B., Lim, H., Carabatsos, M. J., Harrington, A., Ecsedy, J., Pellman, D., Maas, R. and Leder, P. (2002). Formin-2, polyploidy, hypofertility and positioning of the meiotic spindle in mouse oocytes. *Nat. Cell Biol.* **4**, 921-928.

Lee, K. and Rhee, K. (2011). PLK1 phosphorylation of pericentrin initiates centrosome maturation at the onset of mitosis. *J. Cell Biol.* **195**, 1093-1101.

Lister, L. M., Kouznetsova, A., Hyslop, L. A., Kalleas, D., Pace, S. L., Barel, J. C., Nathan, A., Floros, V., Adelfalk, C., Watanabe, Y. et al. (2010). Age-related meiotic segregation errors in mammalian oocytes are preceded by depletion of cohesin and Sgo2. *Curr. Biol.* **20**, 1511-1521.

Lüders, J., Patel, U. K. and Stearns, T. (2006). GCP-WD is a [gamma]-tubulin targeting factor required for centrosomal and chromatin-mediated microtubule nucleation. *Nat. Cell Biol.* **8**, 137-147.

Łuksza, M., Queguigner, I., Verlhac, M.-H. and Brunet, S. (2013). Rebuilding MTOCs upon centriole loss during mouse oogenesis. *Dev. Biol.* **382**, 48-56.

Ma, W. and Viveiros, M. M. (2014). Depletion of pericentrin in mouse oocytes disrupts microtubule organizing center function and meiotic spindle organization. *Mol. Reprod. Dev.* **81**, 1019-1029.

Ma, J., Zeng, F., Schultz, R. M. and Tseng, H. (2006). Basonuclin: a novel mammalian maternal-effect gene. *Development* **133**, 2053-2062.

Ma, W., Baumann, C. and Viveiros, M. M. (2010). NEDD1 is crucial for meiotic spindle stability and accurate chromosome segregation in mammalian oocytes. *Dev. Biol.* **339**, 439.

Manandhar, G., Schatten, H. and Sutovsky, P. (2005). Centrosome reduction during gametogenesis and its significance. *Biol. Reprod.* **72**, 2-13.

Maro, B., Howlett, S. K. and Webb, M. (1985). Non-spindle microtubule organizing centers in metaphase II-arrested mouse oocytes. *J. Cell Biol.* **101**, 1665-1672.

Mennella, V., Keszthelyi, B., McDonald, K. L., Chhun, B., Kan, F., Rogers, G. C., Huang, B. and Agard, D. A. (2012). Subdiffraction-resolution fluorescence microscopy reveals a domain of the centrosome critical for pericentriolar material organization. *Nat. Cell Biol.* **14**, 1159-1168.

Moutinho-Pereira, S., Stuurman, N., Afonso, O., Hornsveld, M., Aguiar, P., Goshima, G., Vale, R. D. and Maiato, H. (2013). Genes involved in centrosome-independent mitotic spindle assembly in Drosophila S2 cells. *Proc. Natl. Acad. Sci. USA* **110**, 19808-19813.

Musacchio, A. and Salmon, E. D. (2007). The spindle-assembly checkpoint in space and time. *Nat. Rev. Mol. Cell Biol.* **8**, 379-393.

Nagaoka, S. I., Hassold, T. J. and Hunt, P. A. (2012). Human aneuploidy: mechanisms and new insights into an age-old problem. *Nat. Rev. Genet.* **13**, 493-504.

Rauch, A., Thiel, C. T., Schindler, D., Wick, U., Crow, Y. J., Ekici, A. B., van Essen, A. J., Goecke, T. O., Al-Gazali, L., Chrzanowska, K. H. et al. (2008). Mutations in the Pericentrin (PCNT) gene cause primordial dwarfism. *Science* **319**, 816-819.

Raynaud-Messina, B. and Merdes, A. (2007). [gamma]-tubulin complexes and microtubule organization. *Curr. Opin. Cell Biol.* **19**, 24-30.

Reber, S. B., Baumgart, J., Widlund, P. O., Pozniakovsky, A., Howard, J., Hyman, A. A. and Jülicher, F. (2013). XMAP215 activity sets spindle length by controlling the total mass of spindle microtubules. *Nat. Cell Biol.* **15**, 1116-1122.

Sathananthan, A. H., Selvaraj, K. and Trounson, A. (2000). Fine structure of human oogonia in the foetal ovary. *Mol. Cell. Endocrinol.* **161**, 3-8.

Schuh, M. and Ellenberg, J. (2007). Self-organization of MTOCs replaces centrosome function during acentrosomal spindle assembly in live mouse oocytes. *Cell* **130**, 484-498.

Stein, P., Svoboda, P. and Schultz, R. M. (2003). Transgenic RNAi in mouse oocytes: a simple and fast approach to study gene function. *Dev. Biol.* **256**, 188-194.

Svoboda, P., Stein, P. and Schultz, R. M. (2001). RNAi in mouse oocytes and preimplantation embryos: effectiveness of hairpin dsRNA. *Biochem. Biophys. Res. Commun.* **287**, 1099-1104.

Szollosi, D., Calarco, P. and Donahue, R. P. (1972). Absence of centrioles in the first and second meiotic spindles of mouse oocytes. *J. Cell Sci.* **11**, 521-541.

Yoshida, S., Kaido, M. and Kitajima, T. S. (2015). Inherent instability of correct kinetochore-microtubule attachments during meiosis I in oocytes. *Dev. Cell* **33**, 589-602.

Yun, Y., Lane, S. I. R. and Jones, K. T. (2013). Premature dyad separation in meiosis II is the major segregation error with maternal age in mouse oocytes. *Development* **141**, 199.

Zimmerman, W. C., Sillibourne, J., Rosa, J. and Doxsey, S. J. (2004). Mitosis-specific anchoring of gamma tubulin complexes by pericentrin controls spindle organization and mitotic entry. *Mol. Biol. Cell* **15**, 3642-3657.